

Improving Accuracy of Internal Combustion Engines Ring Design Tool Using Romberg's Integration and Deferred-Correction Approaches

May 17th 2017

Agenda

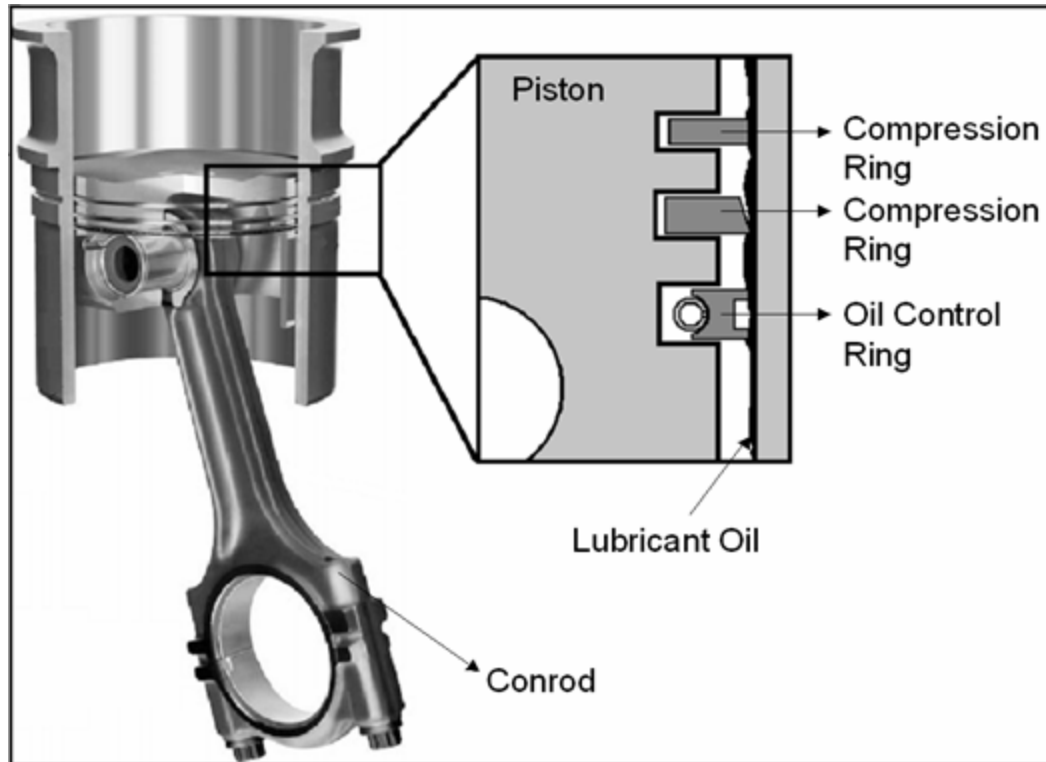
- I. Brief introduction to the ring pack system for internal combustion engines
- II. Conformability analysis using the Curved Beam Based Ring Design Tool
- III. Improving the accuracy of the solution using Romberg's Integration
- IV. Improving the accuracy of the solution using Deferred-Correction Approaches

Conclusion

I. Brief introduction to the ring pack system for internal combustion engines:

Piston rings are metallic seals with an outward expanding strain, that are assembled in the piston. Piston rings have to fulfill three core functions:

- Sealing combustion gases (Blow-by control)
- Controlling oil consumption
- Transferring heat from piston to cylinder



From Mahle

In order to achieve these functions the piston rings must be in contact with the cylinder wall and piston groove side. Typically a ring pack for internal combustion engines consists of three rings:

- first compression ring (also top ring or upper compression ring UCR)
- second compression ring (also second ring or lower compression ring LCR)
- oil control ring OCR (also third ring)

All these functions need to be achieved with low friction and durability. Rings should survive for engine life by means of suitable materials, coatings and designs.

II. Conformability analysis using the Curved Beam Based Ring Design Tool:

Characterize the ring steady state relative position with respect to the groove and the liner

External forces to consider:

- Initial force to close the ring from its free shape to circular one
- Gas pressure forces around the ring
- Asperity contact force with the liner and the groove: Greenwood and Tripp model $P_c =$

$$\begin{cases} 0 & \frac{h}{\sigma} \geq \Omega \\ P_k \left(\Omega - \frac{h}{\sigma} \right)^z & \frac{h}{\sigma} \leq \Omega \end{cases}$$

P_c is the asperity contact pressure, h is the local ring-liner / ring-groove clearance

and σ the standard deviation of the liner / groove surface roughness. P_k depends on the properties of the ring and the liner / groove material. $z = 6.804$ and $\Omega = 4$

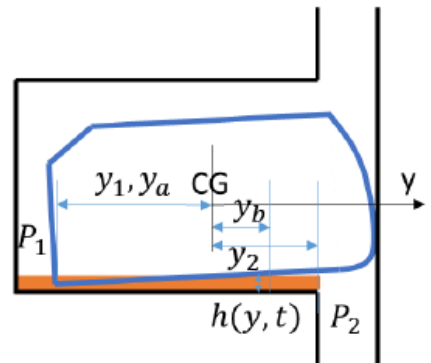
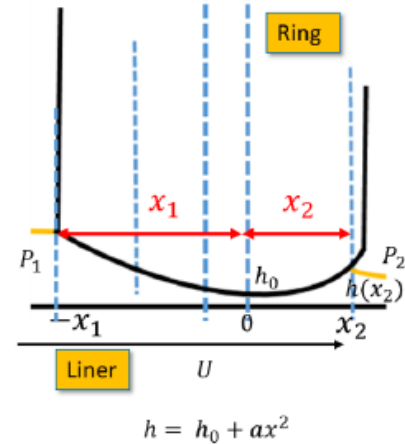
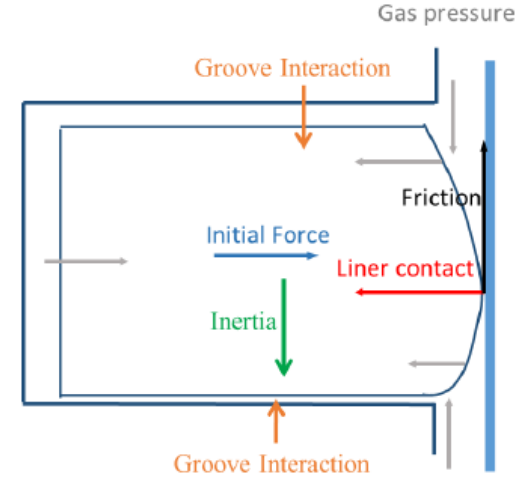
- Liner lubrication forces:

- Partially flooded case: $P_{hydro} = \left(\frac{h_{OCR}}{h_{prof}} \right)^{K_p} \frac{\mu V}{(\mu V)_0} (a_p P_{0,OCR}) \left(\frac{h_{prof}}{\sigma_p} \right)^{-K_{OCR}}$, $\tau_{hydro} = \frac{F_0(\mu V)}{h_{prof}} \left(\frac{h_{OCR}}{h_{prof}} \right)^{K_f}$

- Fully flooded case: $f_{r,hydro} = \frac{12\mu V}{ah_0} c \left(\frac{1 + \tanh\left(\frac{\log_{10}(ax_1^2/h_0) + d}{e}\right)}{2} \right)^b$, $f_{z,hydro} = \int_{-x_1}^{x_2} \frac{\mu V}{h} dx =$
 $\frac{\mu V}{\sqrt{ah_0}} \left[\arctan\left(\sqrt{\frac{a}{h_0}} x_2\right) + \arctan\left(\sqrt{\frac{a}{h_0}} x_1\right) \right]$

- Oil squeezing and ring-groove hydrostatic force: $J(y) = \int_a^y \frac{\partial h}{\partial t} dy'$, $c_1 = \frac{P_d - P_i - 12\mu_{oil} \int_a^b \frac{J(y)}{h^3} dy}{\int_a^b \frac{dy}{h^3}}$

$$f_{oil,gl} = P_d(y_b - y_a) - 12\mu_{oil} \int_a^y \frac{(y-y_a)J(y)}{h^3} dy - c_1 \int_a^b \frac{y-y_a}{h^3} dy, m_{oil,gl} = \frac{P_d(y_b^2 - y_a^2)}{2} - \frac{1}{2} \int_a^b (y - y_a)^2 \frac{\partial P_{oil}}{\partial y} dy$$



Ring's deformations are of the order of $100 \mu m$.

Its length scale is in the order of tens of millimeters.

Ring-liner and ring-groove contact forces depend on the clearances which are within sub-micron level and the on boundary conditions like fuel-lube interaction and bridging which include length scales around $100 \mu m$ and even lower.



To couple local force generation and ring structure deformation, we use a dual grid curved beam finite element method.

Ring structural deformations are solved with sufficient accuracy using a coarse structural mesh and local interactions are studied based on a much finer grid.

For each element: $\frac{\partial L^{(e)}}{\partial u_i^{(e)}} = 0$: Euler-Lagrange equation

$$L^{(e)} = W^{(e)} - U^{(e)}; W^{(e)} = \int_0^{L_e} (f_r y + f_z z + m_t \alpha) ds; U^{(e)} = U_{zz}^{(e)} + U_{yy}^{(e)} + U_{\theta}^{(e)}$$

Under small displacement assumption and for planar deformation:

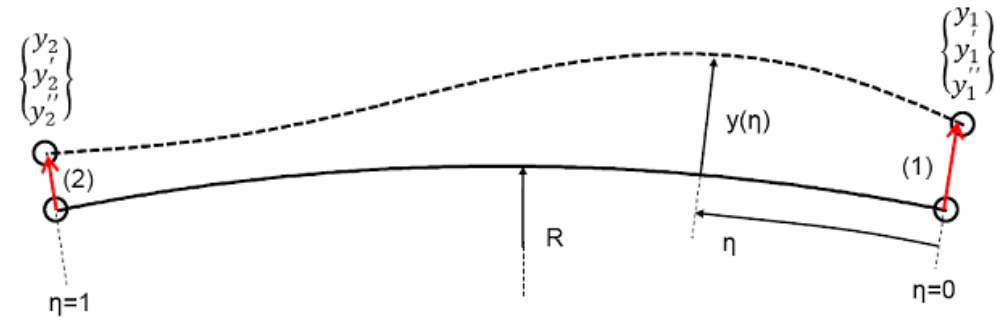
$$U_{zz}^{(e)} = \frac{1}{2} \int_0^{L_e} EI_{zz} (\kappa_{yy} - \kappa_{yy0})^2 ds;$$

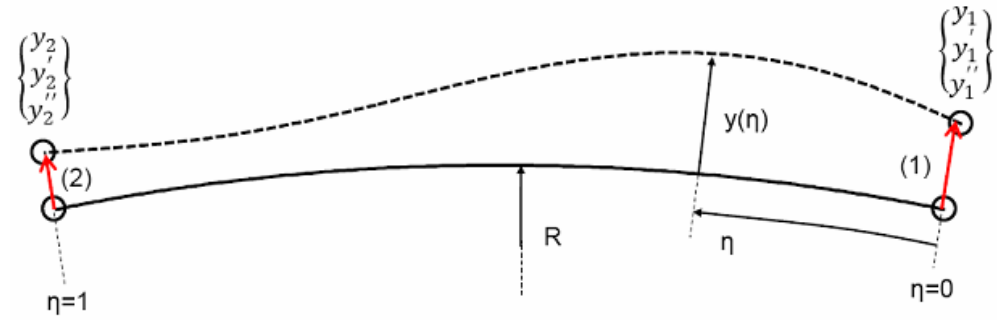
$$U_{yy}^{(e)} = \frac{1}{2} \int_0^{L_e} EI_{yy} (\kappa_{zz} - \kappa_{zz0})^2 ds;$$

$$U_{\theta}^{(e)} = \frac{1}{2} \int_0^{L_e} GJ_t \left(\frac{z' - R\alpha'}{R^2} \right)^2 ds$$

Ring curvature: $\kappa = \frac{1}{R} - \frac{y+y''}{R^2}$

$$\kappa_{yy} = \kappa \cos \left(\alpha + \frac{z''}{R} \right), \kappa_{zz} = \kappa \cos \left(\alpha + \frac{z''}{R} \right)$$





$$u^{(e)} = \{u_1, \dots, u_{16}\} = \{y_1, y_1', y_1'', z_1, z_1', z_1'', \alpha_1, \alpha_1', y_2, y_2', y_2'', z_2, z_2', z_2'', \alpha_2, \alpha_2'\}$$

$$y(\eta) = \sum_{k=1}^6 N_k(\eta) u_{y_k}; z(\eta) = \sum_{k=1}^6 N_k(\eta) u_{z_k}; \alpha(\eta) = \sum_{k=1}^4 N_{\alpha k}(\eta) u_{\alpha k}$$

Under small displacement assumption to linearize the cosine and sine terms:

$$U^{(e)} = \frac{1}{2} \{u\}^{(e)T} [K]^{(e)} \{u\}^{(e)}$$

$$W^{(e)} = \{u\}^{(e)T} \{F_{ext}\}^{(e)}$$

$$F_{initial, k_y}^{(e)} = \frac{\partial U^{(e)}}{\partial u_{k_y}} \Big|_{\substack{y=0, y'=0, y''=0 \\ z=0, z'=0, z''=0 \\ \alpha=\alpha_p, \alpha'=0}}; F_{initial, k_z}^{(e)} = \frac{\partial U^{(e)}}{\partial u_{k_z}} \Big|_{\substack{y=0, y'=0, y''=0 \\ z=0, z'=0, z''=0 \\ \alpha=\alpha_p, \alpha'=0}}; F_{initial, k_\alpha}^{(e)} = \frac{\partial U^{(e)}}{\partial u_{k_\alpha}} \Big|_{\substack{y=0, y'=0, y''=0 \\ z=0, z'=0, z''=0 \\ \alpha=\alpha_p, \alpha'=0}}$$

$[K]^{(e)} \{u\}^{(e)} = \{F_{ext}\}^{(e)} - \{F_{initial}\}^{(e)}$: non linear system of 8. N_{nodes} unknowns to solve

Use Newton-Raphson algorithm

III. Improving the accuracy of the solution using Romberg's Integration:

Third improved solution based on two different mesh size solutions.

$$I_k \approx \frac{4^{p-1}I_{2,k-1} - I_{1,k-1}}{4^{p-1} - 1}$$

$$h_2 = \frac{h_1}{2}$$

$$E(h) = C \cdot h^p + O(h^{p+1})$$

Approximate the ring twist with 5th order polynomial to have the same accuracy for the three coordinates: non linear system of 9. N_{nodes} unknowns to solve.

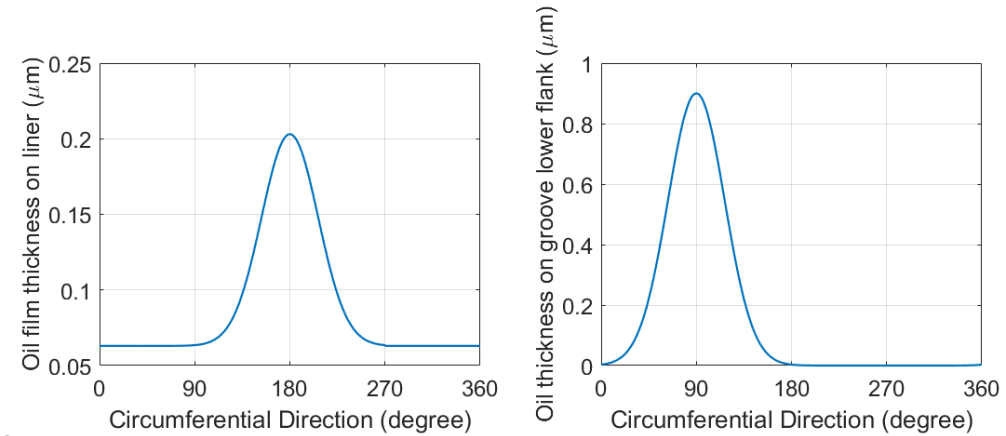
Determine the most appropriate order and the effect of the two mesh sizes.

Compare the average relative error with the one of the finer among the two meshes considered.

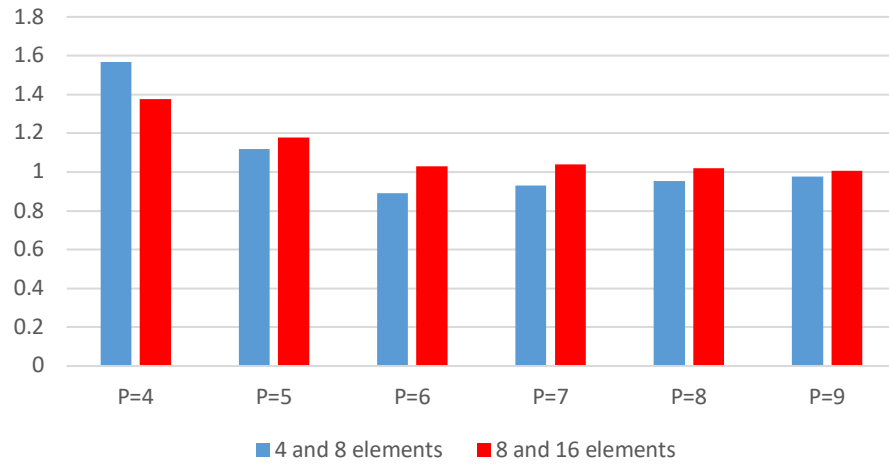
Relative errors are computed by considering the solution obtained with 128 elements as the exact one.

Simulation for a cylinder with $D_b = 95mm$, no bore distortion.

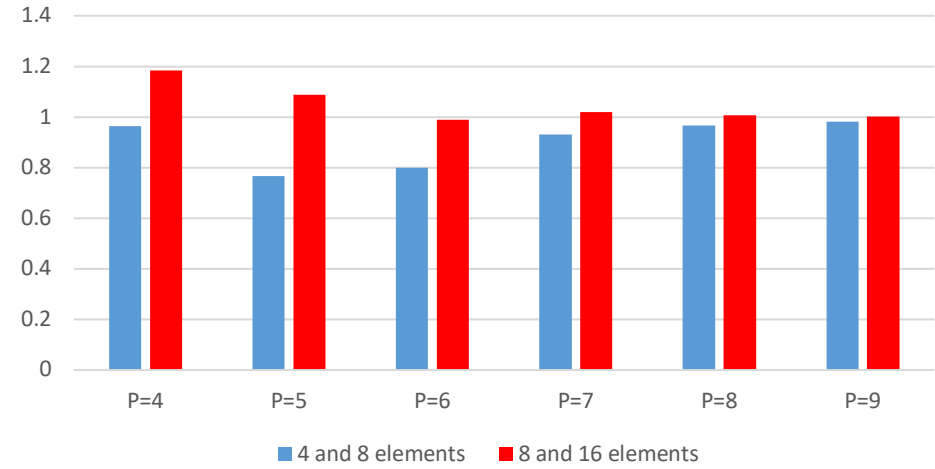
$P_u = P_i = 1.1 \text{ bar}$, $P_d = 1 \text{ bar}$, ring dimensions: 4 by 2 mm



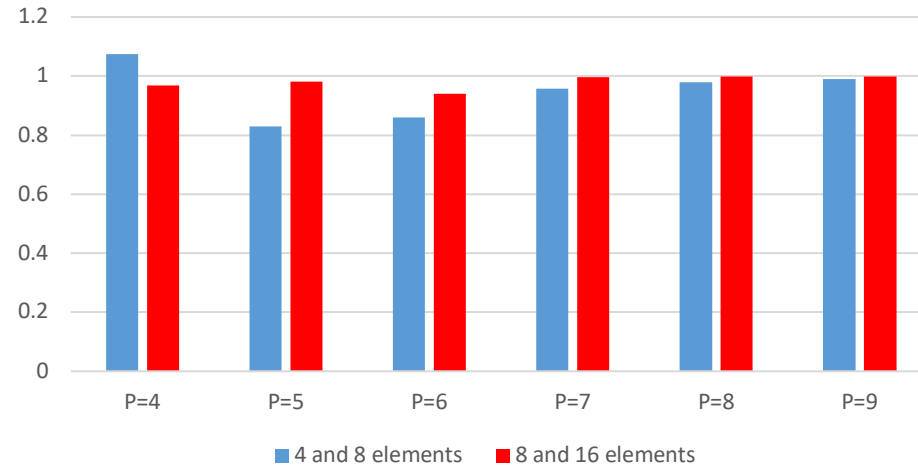
Error ratio for ring liner clearance



Error ratio for axial displacement



Error ratio for static twist



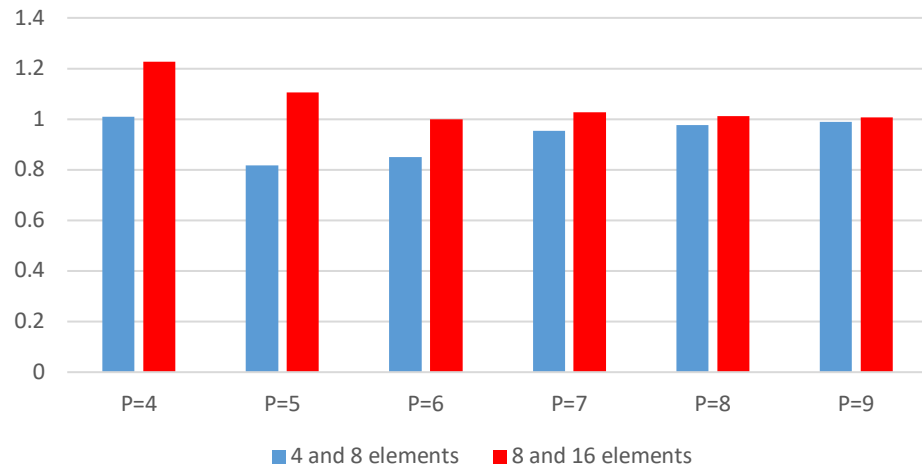
5th order accurate for the coordinate solutions: best result expected for P=6.

Almost always improved solution since we are omitting one term for the error.

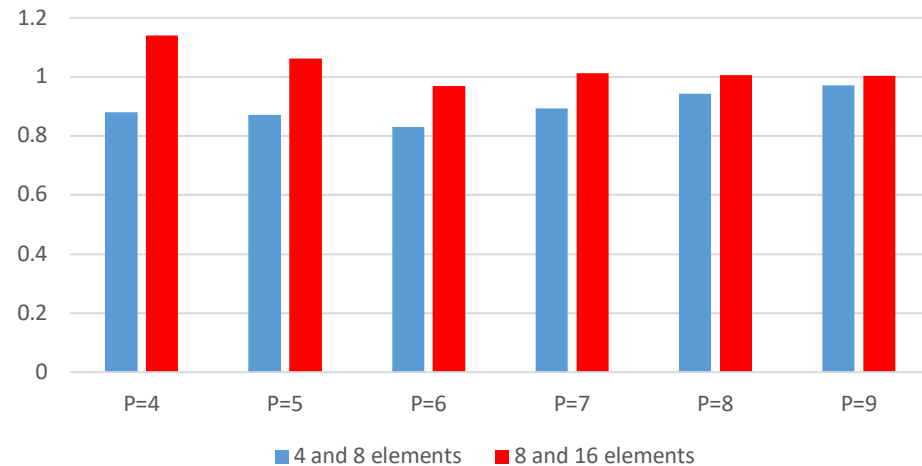
Eliminating higher order terms than the 6th one may be interesting because of the oscillation of the derivatives: shown in the minimum clearance axial location results.

Better improvement of the solution when considering 4 and 8 elements since the term omitted in the residual is bigger.⁸

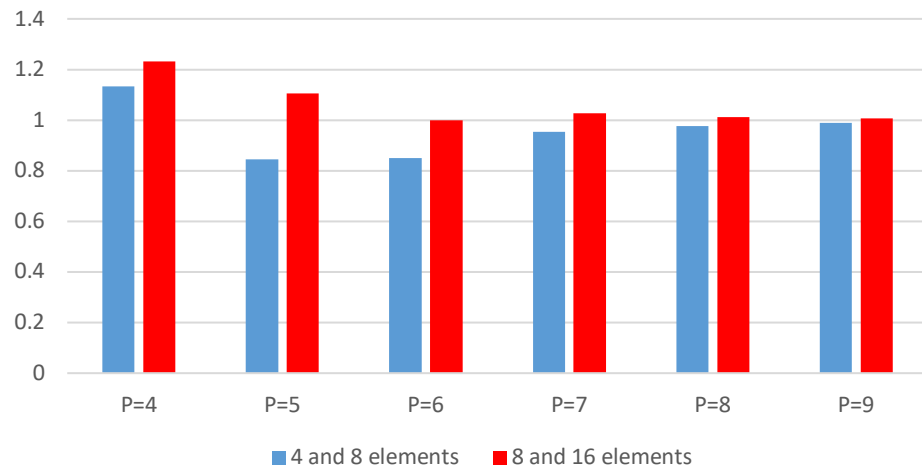
Error ratio for upper OD clearance



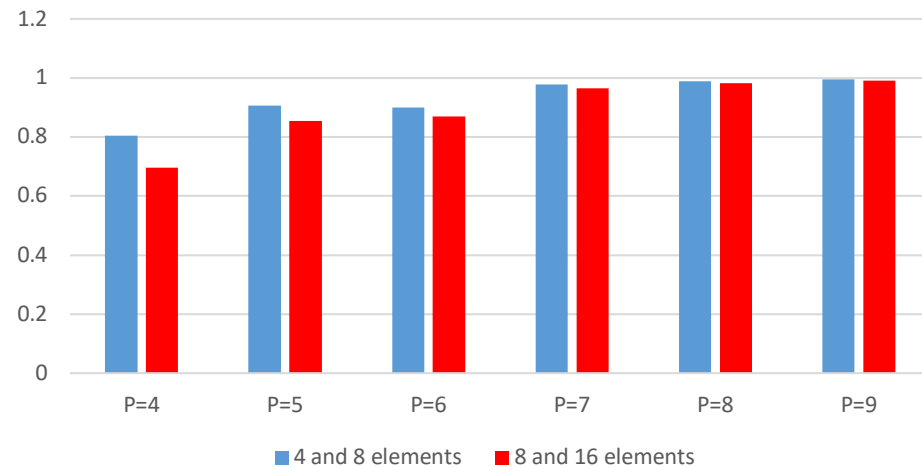
Error ratio for upper ID clearance



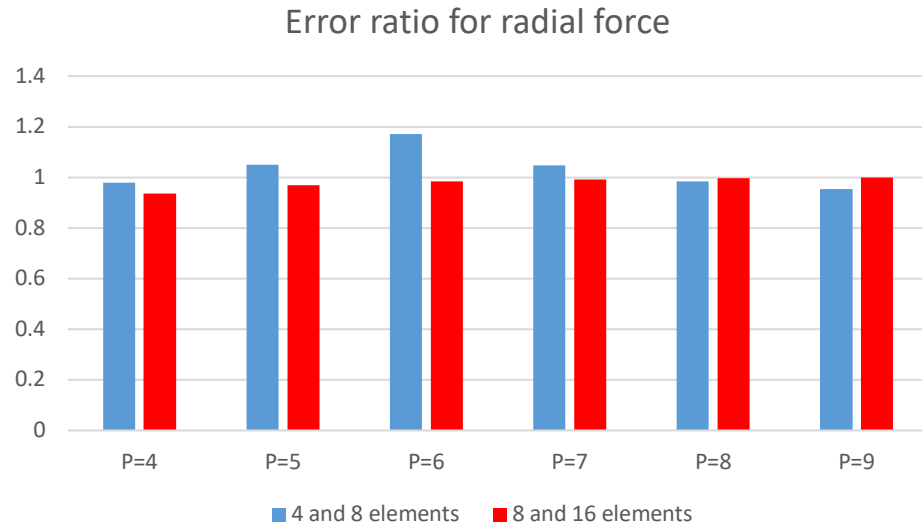
Error ratio for lower OD clearance



Error ratio for lower ID clearance



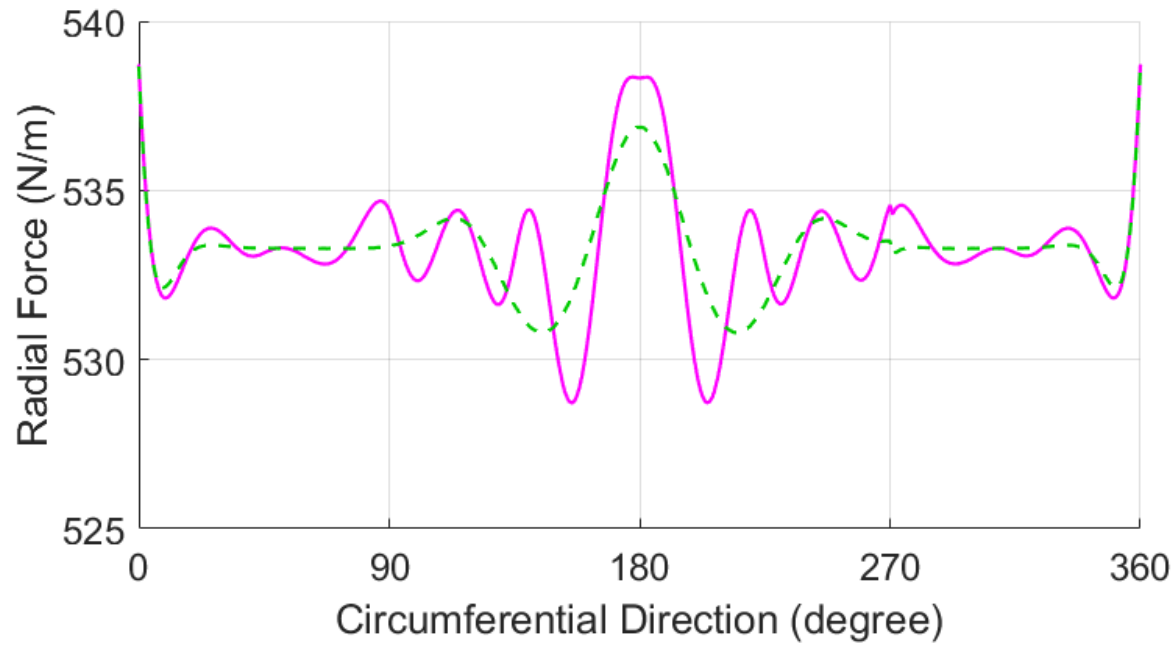
Same trend observed for the upper/lower ID/OD clearances since they linearly depend on the ring coordinate



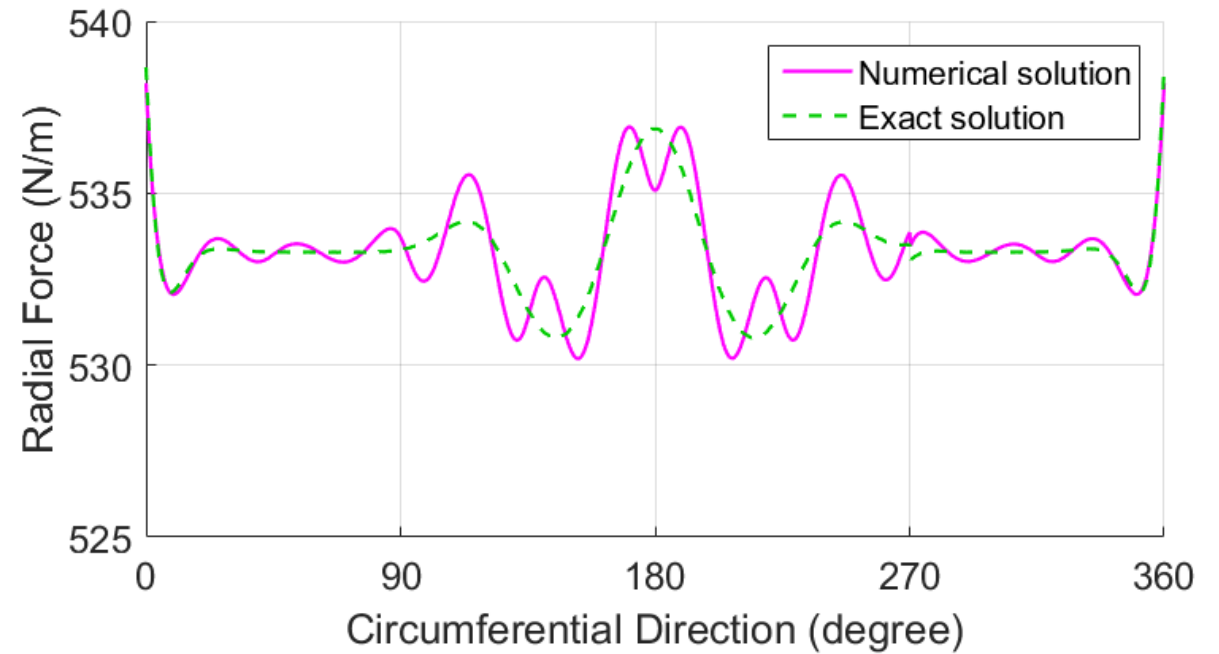
Without Romberg's Integration, we have a less accurate solution (lower order) for the forces and moment distribution.

Romberg's Integration works slightly better for low order correction.

Less efficient than with the ring coordinate solutions.



Using 8 elements



Using 4 and 8 elements with 9th order Romberg's Integration.

VI. Improving the accuracy of the solution using Deferred-Correction Approaches:

Introduce a correction term in the Newton-Raphson iteration based on a finer mesh.

We want to solve a non linear system: $F(x) = 0$

Newton-Raphson iteration: $x_{r+1} = x_r - [JF(x_r)]^{-1}F(x_r)$

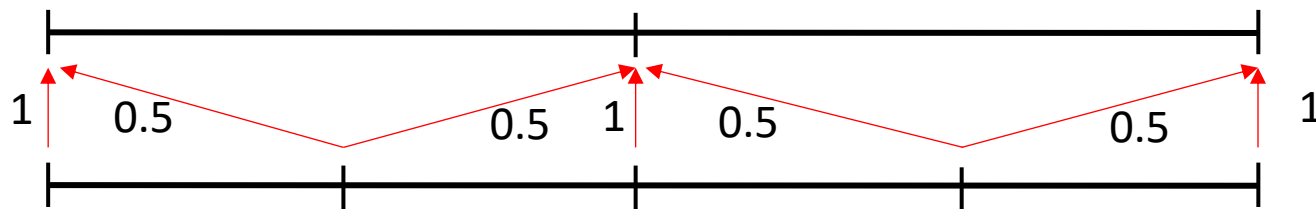
With the correction terms: $x_{r+1} = x_r - [JF(x_r)]^{-1} \left\{ F(x_r) - \omega_1 \left([JF^H(x_r^H)]x_r^H \right)_c - [JF(x_r)]x_r \right\} - \omega_2 \left([F^H(x_r^H)]_c - F(x_r) \right)$

Update x_r^H based on x_r using the shape functions.

How to compute $[JF^H(x_r^H)]x_r^H$ and $[F^H(x_r^H)]_c$ based on $[JF^H(x_r^H)]x_r^H$ and $F^H(x_r^H)$?

-Just pick the values at the corresponding nodes.

-Averaging: what coefficients to use?



Tuning ω_1 and ω_2 to reach convergence for the two methods but less accurate solution than without correction for the same speed of convergence: too high values needed that make the correction terms negligible.

Conclusion

- Romberg's Integration method improved the accuracy of our model specially for the ring coordinate results.
- Better improvement when merging finer meshes.
- Need to consider lower order correction for the force and moment distribution since our solution is less accurate for those results than for the ring coordinates.

- Fail to improve the accuracy of our model using Deferred-Correction approaches applied to Newton-Raphson algorithm.
- Need to reconsider the averaging when computing $[JF^H(x_r^H)]x_r^H$ and $[F^H(x_r^H)]_c$ from $[JF(x_r)]x_r$ and $F(x_r)$ by looking at the 'physical' meaning of those terms when solving: $[K]\{u\} = \{F_{ext}\} - \{F_{initial}\}$ with $U^{(e)} = \frac{1}{2}\{u\}^{(e)T} [K]^{(e)}\{u\}^{(e)}$.

Thank you for your attention

Questions?
Solutions?